



# Robust second-order accurate discretizations of the multi-dimensional Heaviside and Dirac delta functions

Chohong Min<sup>a</sup>, Frédéric Gibou<sup>b,c,\*</sup>

<sup>a</sup> Mathematics Department and Research Institute for Basic Sciences, KyungHee University, Seoul 130-701, Republic of Korea

<sup>b</sup> Department of Mechanical Engineering, University of California, Santa Barbara, CA 93106, United States

<sup>c</sup> Department of Computer Science, University of California, Santa Barbara, CA 93106, United States

## ARTICLE INFO

### Article history:

Received 13 November 2007

Received in revised form 19 July 2008

Accepted 23 July 2008

Available online 14 August 2008

### Keywords:

Heaviside function

Dirac delta function

Level set methods

Singular source term

## ABSTRACT

We present a robust second-order accurate method for discretizing the multi-dimensional Heaviside and the Dirac delta functions on irregular domains. The method is robust in the following ways: (1) integrations of source terms on a co-dimension one surface are independent of the underlying grid and therefore stable under perturbations of the domain's boundary; (2) the method depends only on the function value of a level function, not on its derivatives. We present the discretizations in tabulated form to make their implementations straightforward. We present numerical results in two and three spatial dimensions to demonstrate the second-order accuracy in the  $L^1$ -norm in the case of the solution of PDEs with singular source terms. In the case of evaluating the contribution of singular source terms on interfaces, the method is also second-order accurate in the  $L^\infty$ -norm.

© 2008 Elsevier Inc. All rights reserved.

## 1. Introduction

The use of regularized Heaviside and delta functions is ubiquitous in computational science and provide a systematic framework to discretize source terms and to approximate discontinuous variables on irregular domains. For example, the numerical approximations of the Heaviside and delta functions are widely used in the level set community to discretize two-phase flow problems and to evaluate singular source terms such as surface tension forces, as introduced by Sussman et al. [22] in the context of two-phase flows. Volume of fluid, Front Tracking, Immersed Boundary and Phase-Field methods also use a smear-out approach where the discretization of the Heaviside and delta can be handy (see for example [26,2,7,15] and the references therein). In addition, several hybridizations of numerical methods have been proposed, such as particle/level set [5] and VOF/levelset [21], so that the use of numerical delta and Heaviside functions is omnipresent in computational science and engineering.

More precisely, consider an irregular domain  $\Omega \subset \mathbb{R}^d$  and its boundary  $\Gamma = \partial\Omega$ . Here, the sets are assumed to be represented through a level function  $\phi : \mathbb{R}^d \rightarrow \mathbb{R}$  as

$$\Omega = \{x \in \mathbb{R}^d \mid \phi(x) \leq 0\},$$

$$\Gamma = \{x \in \mathbb{R}^d \mid \phi(x) = 0\}.$$

We note that in the case where  $\Omega$  and  $\Gamma$  are not described by a level function, as it is the case for front-tracking, volume of fluid, or phase-field methods, a signed distance function to  $\Gamma$  can be constructed using any of the well-documented algorithms, such as [17,14,19,13]. Therefore, our discretizations are not limited to level set methods.

\* Corresponding author. Address: Department of Mechanical Engineering, University of California, Santa Barbara, CA 93106, United States. Tel.: +1 8058937152.

E-mail address: [fgibou@engineering.ucsb.edu](mailto:fgibou@engineering.ucsb.edu) (F. Gibou).

Using this functional representation, one can compute integrals on irregular domains  $\Omega$  or interfaces  $\Gamma$  as integrals on regular domains as

$$\int_{\Omega} f \, d\Omega = \int_{\mathbb{R}^d} f(x) \cdot H(\phi(x)) \, dx,$$

$$\int_{\Gamma} f \, d\Gamma = \int_{\mathbb{R}^d} f(x) \cdot \delta(\phi(x)) \cdot \|\nabla(\phi(x))\| \, dx.$$

Several approximations of the one-dimensional delta and Heaviside functions have been proposed in the literature, see [14,18] for a review. However, Tornberg and Engquist [23] pointed out that the standard approximations used in the level set community may lead to erroneous results and provided an example where, even in the simple computation of the length of a curve, the use of standard numerical delta functions could lead to non-convergent approximations. Later, Engquist et al. [4] proposed first-order accurate discretizations of the Dirac delta function that removes the problem of convergence. We note that they also proposed a second-order accurate discretization of delta, but that only two-dimensional results are presented, possibly because of its complexity. Also, leveraging on the work of Mayo [9] and building on the work of Calhoun and Smereka [3], Smereka proposed first- and second-order accurate discretizations of the regularized delta function and proposed numerical results using the computation of length and areas of irregular domains to demonstrate their accuracy [20]. In this work, the discretization of the Dirac delta involves second-order derivatives of a level set function, which may lead to numerical noise. Discretization of Dirac delta involving derivatives of functions can also be found in the work of Towers [24,25]. We also note that the interesting work of Walén [27] addresses discretizations of Dirac delta, although only treating the one-dimensional case. In Min and Gibou [12], we proposed a second-order accurate geometric approach to the computation of length and area that is robust to the perturbations of the irregular domain’s boundary. However, this work focused only on approximating integrals for computing lengths, areas and volumes of irregular domains and did not provide explicit discretizations of Heaviside and delta functions.

In this paper, integrals over irregular domains are first converted to integrals over regular domains via the multi-dimensional Heaviside and delta functions:

$$\int_{\Omega} f \, d\Omega = \int_{\mathbb{R}^d} f(x) \cdot H_{\Omega}(x) \, dx \quad \text{and} \quad \int_{\Gamma} f \, d\Gamma = \int_{\mathbb{R}^d} f(x) \cdot \delta_{\Gamma}(x) \, dx,$$

then, leveraging on the robust geometric integration of [12], we propose a direct discretizations  $\delta_{ij}$  and  $H_{ij}$  of the multi-dimensional Heaviside and delta functions in two and three spatial dimensions such that:

$$\int_{\Omega} f \, d\Omega = \sum_{ij} H_{ij} \cdot f_{ij} \Delta x \Delta y + O(\Delta x^2 + \Delta y^2) \tag{1}$$

and

$$\int_{\Gamma} f \, d\Gamma = \sum_{ij} \delta_{ij} \cdot f_{ij} \Delta x \Delta y + O(\Delta x^2 + \Delta y^2). \tag{2}$$

We first consider discretizing the integrals over irregular domains. Then discretizations of the multi-dimensional Heaviside and delta functions will follow from the discretizations of Eqs. (1) and (2).

## 2. Geometric integration

In [10], an isosurfacing method was introduced to efficiently decompose the irregular domains  $\Omega$  and  $\Gamma$  defined by the level function  $\phi$  into simplices. Using the quadrature rules on simplices (triangles in 2D and tetrahedra in 3D), we proposed in [12] an efficient and second-order accurate integration method. In addition, we showed that this method is robust to the perturbation of the interface on the underlying grid. For the sake of clarity, we briefly review next the integration method.

On Cartesian grids, we assume that the level function  $\phi$  and the integrand  $f$  are sampled at grid nodes. Each grid cell can be decomposed into simplices and the integrals can be evaluated as the sum over the simplices. It is enough then to consider integration over one simplex, as described next.

### 2.1. Two spatial dimensions

Consider a triangle with vertices  $P_1, P_2$  and  $P_3$ , denoted  $\Delta P_0 P_1 P_2$ , to be an element in the decomposition of a two-dimensional domain. We denote by  $\phi_i$  and  $f_i$ , the values of the level function and the integrand function on a vertex  $P_i$ . Whenever  $\phi_i \phi_j < 0$ , there exists an interface point on the line segment  $\overline{P_i P_j}$ , which we denote by  $P_{ij}$  and approximated by linear interpolation:

$$P_{ij} = P_i \frac{\phi(P_j)}{\phi(P_j) - \phi(P_i)} + P_j \frac{\phi(P_i)}{\phi(P_i) - \phi(P_j)}.$$

Using the interface points, the intersections of the irregular domain  $\Omega$  and interface  $\Gamma$  with the triangle are discretized as

$$\Omega \cap \Delta P_0 P_1 P_2 = \begin{cases} \Delta P_0 P_1 P_2 & \text{if } \phi_0, \phi_1, \phi_2 < 0 \\ \Delta P_0 P_1 P_{02} \cup \Delta P_{12} P_1 P_{02} & \text{if } \phi_0, \phi_1 < 0 \text{ and } \phi_2 > 0 \\ \Delta P_{02} P_{12} P_2 & \text{if } \phi_0 < 0 \text{ and } \phi_1, \phi_2 > 0 \\ \emptyset & \text{if } \phi_0, \phi_1, \phi_2 > 0 \end{cases}$$

and

$$\Gamma \cap \Delta P_0 P_1 P_2 = \begin{cases} \emptyset & \text{if } \phi_0, \phi_1, \phi_2 < 0 \\ \overline{P_{02} P_{12}} & \text{if } \phi_0, \phi_1 < 0 \text{ and } \phi_2 > 0 \\ \overline{P_{02} P_{01}} & \text{if } \phi_0 < 0 \text{ and } \phi_1, \phi_2 > 0 \\ \emptyset & \text{if } \phi_0, \phi_1, \phi_2 > 0 \end{cases}$$

as depicted in Fig. 1.

Note: Without loss of generality, we assumed that the values of  $\phi_0, \phi_1,$  and  $\phi_2$  were sorted with the negative signs first. Note also that  $\Omega \cap \Delta P_0 P_1 P_2$  and  $\Gamma \cap \Delta P_0 P_1 P_2$  are now the union of simplices. On each simplex of the irregular domains, one can apply the midpoint quadrature rule to approximate the contribution of the integral of  $f$  over that simplex. For example, in the case where  $\phi_0, \phi_1 < 0$  and  $\phi_2 > 0$ , we have:

$$\int_{\Omega \cap \Delta P_0 P_1 P_2} f \, d\Omega = \int_{\Delta P_0 P_1 P_{02}} f \, d\Omega + \int_{\Delta P_{12} P_1 P_{02}} f \, d\Omega \approx \frac{1}{3} (f(P_0) + f(P_1) + f(P_{02})) A(P_0 P_1 P_{02}) + \frac{1}{3} (f(P_{12}) + f(P_1) + f(P_{02})) A(P_{12} P_1 P_{02})$$

and

$$\int_{\Gamma \cap \Delta P_0 P_1 P_2} f \, d\Gamma = \int_{\Delta P_{02}} P_{12} f \, d\Gamma \approx \frac{1}{2} (f(P_{02}) + f(P_{12})) L(P_{02} P_{12}),$$

where  $A(P_i P_j P_k)$  and  $L(P_i P_j)$  denote the area of the triangle  $\Delta P_i P_j P_k$  and the length of the line segment  $\overline{P_i P_j}$ , respectively. Since  $f$  is only sampled on grid nodes, the unknown value  $f(P_{ij})$  is simply linearly interpolated as

$$f(P_{ij}) = \frac{f_i \phi_j - f_j \phi_i}{\phi_j - \phi_i}.$$

The integrals above thus become:

$$\int_{\Omega \cap \Delta P_0 P_1 P_2} f \, d\Omega \approx \frac{A(P_0 P_1 P_{02})}{3} \left( f_0 + f_1 + \frac{f_0 \phi_2 - f_2 \phi_0}{\phi_2 - \phi_0} \right) + \frac{A(P_{12} P_1 P_{02})}{3} \left( \frac{f_1 \phi_2 - f_2 \phi_1}{\phi_2 - \phi_1} + f_1 + \frac{f_0 \phi_2 - f_2 \phi_0}{\phi_2 - \phi_0} \right)$$

and

$$\int_{\Gamma \cap \Delta P_0 P_1 P_2} f \, d\Gamma \approx \frac{L(P_{02} P_{12})}{2} \left( \frac{f_0 \phi_2 - f_2 \phi_0}{\phi_2 - \phi_0} + \frac{f_1 \phi_2 - f_2 \phi_1}{\phi_2 - \phi_1} \right).$$

The above discretizations are linear polynomials with respect to the sampled function values  $f_0, f_1,$  and  $f_2$ , which we write as

$$\begin{aligned} \int_{\Omega \cap \Delta P_0 P_1 P_2} f \, d\Omega &\approx f_0 H_0 + f_1 H_1 + f_2 H_2, \\ \int_{\Gamma \cap \Delta P_0 P_1 P_2} f \, d\Gamma &\approx f_0 \delta_0 + f_1 \delta_1 + f_2 \delta_2, \end{aligned} \tag{3}$$

where the  $H_i$ 's and  $\delta_i$ 's are the coefficients of the linear polynomials  $f_i$ 's. Note that these coefficients are functions of the six arguments  $\phi_0, \phi_1, \phi_2, P_0, P_1$  and  $P_2$  and that the discretizations in (3) does not depend on the order of indexing of the vertices. Therefore, once one of the coefficients, say  $H_0(\phi_0, \phi_1, \phi_2, P_0, P_1, P_2)$ , is known, the other coefficients directly follow it, i.e.:

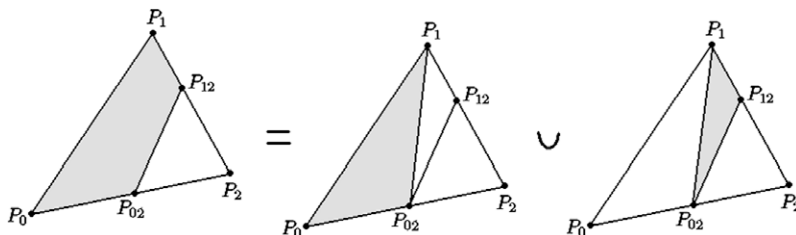


Fig. 1. Decomposition of the frustum  $P_0 P_{02} P_{12} P_1$  of a triangle  $P_0 P_1 P_2$  into two simplices  $P_0 P_{02} P_1$  and  $P_{02} P_{12} P_1$ .

**Table 1**  
Formulas for the discretization of  $H_0$  and  $\delta_0$  in two spatial dimensions

$\phi_0$	$\phi_1$	$\phi_2$	$H_0(\phi_0, \phi_1, \phi_2, P_0, P_1, P_2)$	$\delta_0(\phi_0, \phi_1, \phi_2, P_0, P_1, P_2)$
—	—	—	$\frac{A(P_0P_1P_2)}{3}$	0
—	—	+	$\frac{A(P_0P_1P_2)}{3} - \frac{A(P_{02}P_{12}P_2)}{3} \cdot \frac{\phi_2}{\phi_2 - \phi_0}$	$\frac{L(P_{02}P_{12})}{2} \cdot \frac{\phi_2}{\phi_2 - \phi_0}$
—	+	—	$\frac{A(P_0P_1P_2)}{3} - \frac{A(P_{01}P_{21}P_1)}{3} \cdot \frac{\phi_1}{\phi_1 - \phi_0}$	$\frac{L(P_{01}P_{21})}{2} \cdot \frac{\phi_1}{\phi_1 - \phi_0}$
—	+	+	$\frac{A(P_{01}P_{02}P_0)}{3} \cdot (1 + \frac{\phi_2}{\phi_2 - \phi_0} + \frac{\phi_1}{\phi_1 - \phi_0})$	$\frac{L(P_{01}P_{02})}{2} \cdot (\frac{\phi_1}{\phi_1 - \phi_0} + \frac{\phi_2}{\phi_2 - \phi_0})$

Note that  $\delta(\phi) = \delta(-\phi)$  and that  $H(-\phi) = A(P_0, P_1, P_2) - H(\phi)$ .

$$H_1(\phi_0, \phi_1, \phi_2, P_0, P_1, P_2) = H_0(\phi_1, \phi_0, \phi_2, P_1, P_0, P_2)$$

and

$$H_2(\phi_0, \phi_1, \phi_2, P_0, P_1, P_2) = H_0(\phi_2, \phi_0, \phi_1, P_2, P_0, P_1).$$

As a consequence, it is enough to derive formulas for  $H_0$  and  $\delta_0$ , which we give in Table 1. These formulas depend on the sign of the  $\phi$  since the combination of signs define the location and geometry of the domain and of the interface.

2.2. Extension to three spatial dimensions

The integration method presented above can be extended to three spatial dimensions in the same fashion by first triangulating the grid into simplices. In this case, among the many possible decompositions, two choices are evident: each grid cell can be decomposed in either five tetrahedra (the middle cut triangulation [16]) or into six tetrahedra (the Kuhn triangulation [8]) as illustrated in Fig. 2. The advantage of the Kuhn triangulation is that it can be more easily extended to higher spatial dimensions, as described in [10]. It is also a better choice if one needs to match triangulations between adjacent cells [6]. The advantage of the middle cut triangulation is that the angles of the tetrahedra are less acute than those of the Kuhn triangulation and that the total number of tetrahedra is less, which is preferable for computational efficiency. We choose the middle cut triangulation since we do not need to consider interactions between adjacent cells and limit ourselves to two and three spatial dimensions. The simplicity of this decomposition also translates to the simplicity of the method.

Then, given a tetrahedra  $\Delta P_0P_1P_2P_3$ , the irregular domains  $\Omega \cap \Delta P_0P_1P_2P_3$  and  $\Gamma \cap \Delta P_0P_1P_2P_3$  are decomposed into a disjoint union of tetrahedra and triangles, respectively, as depicted in Figs. 3 and 4. By using the midpoint quadrature rule on tetrahedra and triangles, we obtain the following second-order accurate integration approximations:

$$\int_{\Omega \cap \Delta P_0P_1P_2P_3} f \, d\Omega \approx f_0H_0 + f_1H_1 + f_2H_2 + f_3H_3, \tag{4}$$

$$\int_{\Gamma \cap \Delta P_0P_1P_2P_3} f \, d\Gamma \approx f_0\delta_0 + f_1\delta_1 + f_2\delta_2 + f_3\delta_3.$$

Similarly to the two-dimensional case, the coefficients  $H_i$ 's and  $\delta_i$ 's are functions of the eight arguments  $\phi_0, \phi_1, \phi_2, \phi_3, P_0, P_1, P_2$  and  $P_3$ , and can be expressed as a function of each others. For example, one can define  $H_1, H_2$  and  $H_3$  as

$$H_1(\phi_0, \phi_1, \phi_2, \phi_3, P_0, P_1, P_2, P_3) = H_0(\phi_1, \phi_0, \phi_2, \phi_3, P_1, P_0, P_2, P_3),$$

$$H_2(\phi_0, \phi_1, \phi_2, \phi_3, P_0, P_1, P_2, P_3) = H_0(\phi_2, \phi_0, \phi_1, \phi_3, P_2, P_0, P_1, P_3),$$

$$H_3(\phi_0, \phi_1, \phi_2, \phi_3, P_0, P_1, P_2, P_3) = H_0(\phi_3, \phi_0, \phi_1, \phi_2, P_3, P_0, P_1, P_2).$$

Table 2 presents the formula for  $H_0$  and  $\delta_0$  in three spatial dimensions.

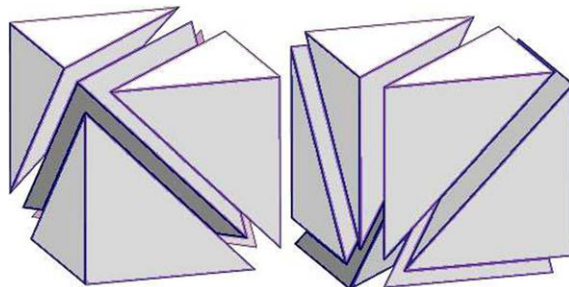


Fig. 2. Middle cut triangulation (left) and Kuhn triangulation (right) of a three-dimensional grid cell.

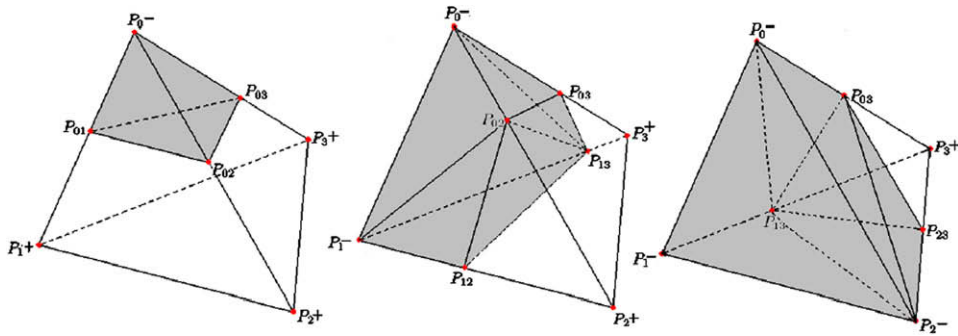


Fig. 3. The three generic representations of the set  $S \cap \Omega$ , where  $S$  is a simplex in three spatial dimensions (i.e. a tetrahedron): one tetrahedron (left) or the union of three tetrahedra (center and right).

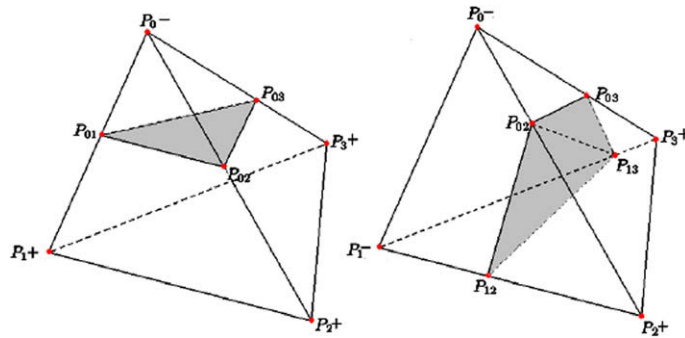


Fig. 4. Generic cases of the decomposition of  $S \cap \Gamma$ , where  $S$  is a simplex in three spatial dimensions:  $S \cap \Gamma \approx \text{conv}(\{P_{ij} | \phi(P_i)\phi(P_j) < 0\})$ .

Table 2  
Formulas for the discretization of  $H_0$  in three spatial dimensions

$\phi_0$	$\phi_1$	$\phi_2$	$\phi_3$	$H_0(\phi_0, \phi_1, \phi_2, \phi_3, P_0, P_1, P_2, P_3)$	$\delta_0(\phi_0, \phi_1, \phi_2, \phi_3, P_0, P_1, P_2, P_3)$
-	-	-	-	$\frac{V(P_0P_1P_2P_3)}{4}$	0
-	-	-	+	$\frac{V(P_0P_1P_2P_3)}{4} - \frac{V(P_{03}P_{13}P_{23}P_3)}{4} \frac{\phi_3}{\phi_3 - \phi_0}$	$\frac{A(P_{03}P_{13}P_{23})}{3} \frac{\phi_3}{\phi_3 - \phi_0}$
-	-	+	-	$\frac{V(P_0P_1P_2P_3)}{4} - \frac{V(P_{02}P_{12}P_{23}P_3)}{4} \frac{\phi_2}{\phi_2 - \phi_0}$	$\frac{A(P_{02}P_{12}P_{23})}{3} \frac{\phi_2}{\phi_2 - \phi_0}$
-	-	+	+	$\frac{V(P_0P_{02}P_{03}P_{13})}{4} (1 + \frac{\phi_2}{\phi_2 - \phi_0} + \frac{\phi_3}{\phi_3 - \phi_0}) + \frac{V(P_0P_{02}P_1P_{13})}{4} (1 + \frac{\phi_2}{\phi_2 - \phi_0}) + \frac{V(P_{02}P_1P_{12}P_{13})}{4} \frac{\phi_2}{\phi_2 - \phi_0}$	$\frac{A(P_{02}P_{03}P_{13})}{3} (\frac{\phi_2}{\phi_2 - \phi_0} + \frac{\phi_3}{\phi_3 - \phi_0}) + \frac{A(P_{02}P_{12}P_{13})}{3} \frac{\phi_2}{\phi_2 - \phi_0}$
-	+	-	-	$\frac{V(P_0P_1P_2P_3)}{4} - \frac{V(P_0P_1P_{12}P_{13})}{4} \frac{\phi_1}{\phi_1 - \phi_0}$	$\frac{A(P_0P_{12}P_{13})}{3} \frac{\phi_1}{\phi_1 - \phi_0}$
-	+	-	+	$\frac{V(P_0P_{01}P_{03}P_{23})}{4} (1 + \frac{\phi_1}{\phi_1 - \phi_0} + \frac{\phi_3}{\phi_3 - \phi_0}) + \frac{V(P_0P_{01}P_2P_{23})}{4} (1 + \frac{\phi_1}{\phi_1 - \phi_0}) + \frac{V(P_{01}P_{12}P_2P_{23})}{4} \frac{\phi_1}{\phi_1 - \phi_0}$	$\frac{A(P_0P_{03}P_{23})}{3} (\frac{\phi_1}{\phi_1 - \phi_0} + \frac{\phi_3}{\phi_3 - \phi_0}) + \frac{A(P_{01}P_{12}P_{23})}{3} \frac{\phi_1}{\phi_1 - \phi_0}$
-	+	+	-	$\frac{V(P_0P_{01}P_{02}P_{23})}{4} (1 + \frac{\phi_1}{\phi_1 - \phi_0} + \frac{\phi_2}{\phi_2 - \phi_0}) + \frac{V(P_0P_{01}P_{23}P_3)}{4} (1 + \frac{\phi_1}{\phi_1 - \phi_0}) + \frac{V(P_{01}P_{13}P_{23}P_3)}{4} \frac{\phi_1}{\phi_1 - \phi_0}$	$\frac{A(P_0P_{02}P_{23})}{3} (\frac{\phi_1}{\phi_1 - \phi_0} + \frac{\phi_2}{\phi_2 - \phi_0}) + \frac{A(P_{01}P_{13}P_{23})}{3} \frac{\phi_1}{\phi_1 - \phi_0}$
-	+	+	+	$\frac{V(P_0P_{01}P_{02}P_{03})}{4} (1 + \frac{\phi_1}{\phi_1 - \phi_0} + \frac{\phi_2}{\phi_2 - \phi_0})$	$\frac{A(P_{01}P_{02}P_{03})}{3} (\frac{\phi_1}{\phi_1 - \phi_0} + \frac{\phi_2}{\phi_2 - \phi_0} + \frac{\phi_3}{\phi_3 - \phi_0})$

Note that  $\delta(\phi) = \delta(-\phi)$  and that  $H(-\phi) = V(P_0, P_1, P_2, P_3) - H(\phi)$ .

### 3. Discretization of the multi-dimensional Heaviside and delta functions

Eq. (1) gives a relationship between a discretization of the multi-dimensional Heaviside function and an approximation of  $\int_{\Omega} f d\Omega$ . Therefore, using the robust second-order accurate discretizations of  $\int_{\Omega} f d\Omega$  described in Section 2, we obtain a robust second-order accurate discretization of the multi-dimensional Heaviside functions. Likewise, Eq. (2) gives a relationship between a discretization of the multi-dimensional delta function and an approximation of  $\int_{\Gamma} f d\Gamma$ . Therefore, a robust second-order accurate of the delta function can be given in terms of the integration method of Section 2.

#### 3.1. Two spatial dimensions

Consider a Cartesian grid with spacing  $\Delta x$  and  $\Delta y$  in the  $x$ - and  $y$ -direction, respectively. We use the standard notation of  $x_i = i\Delta x$  and  $y_j = j\Delta y$  and we write:

$$\int_{\Omega} f \, d\Omega = \sum_{ij} \int_{\Omega \cap [x_i, x_{i+1}] \times [y_j, y_{j+1}]} f \, dx = \sum_{ij} \int_{\Omega \cap \Delta P_{ij} P_{i+1j} P_{i+1j+1}} f \, dx + \sum_{ij} \int_{\Omega \cap \Delta P_{ij} P_{ij+1} P_{i+1j+1}} f \, dx.$$

Using the geometric integration of Section 2 on each term, we have:

$$\int_{\Omega} f \, d\Omega \approx \sum_{ij} \begin{pmatrix} f_{ij} & H_0(\phi_{ij}, \phi_{i+1j}, \phi_{i+1j+1}, P_{ij}, P_{i+1j}, P_{i+1j+1}) \\ +f_{i+1j} & H_1(\phi_{ij}, \phi_{i+1j}, \phi_{i+1j+1}, P_{ij}, P_{i+1j}, P_{i+1j+1}) \\ +f_{i+1j+1} & H_2(\phi_{ij}, \phi_{i+1j}, \phi_{i+1j+1}, P_{ij}, P_{i+1j}, P_{i+1j+1}) \\ +f_{ij} & H_0(\phi_{ij}, \phi_{ij+1}, \phi_{i+1j+1}, P_{ij}, P_{ij+1}, P_{i+1j+1}) \\ +f_{ij+1} & H_1(\phi_{ij}, \phi_{ij+1}, \phi_{i+1j+1}, P_{ij}, P_{ij+1}, P_{i+1j+1}) \\ +f_{i+1j+1} & H_2(\phi_{ij}, \phi_{ij+1}, \phi_{i+1j+1}, P_{ij}, P_{ij+1}, P_{i+1j+1}) \end{pmatrix},$$

which we can write in terms of  $H_0$  as

$$\int_{\Omega} f \, d\Omega \approx \sum_{ij} \begin{pmatrix} f_{ij} & H_0(\phi_{ij}, \phi_{i+1j}, \phi_{i+1j+1}, P_{ij}, P_{i+1j}, P_{i+1j+1}) \\ +f_{i+1j} & H_0(\phi_{i+1j}, \phi_{ij}, \phi_{i+1j+1}, P_{i+1j}, P_{ij}, P_{i+1j+1}) \\ +f_{i+1j+1} & H_0(\phi_{i+1j+1}, \phi_{ij}, \phi_{i+1j}, P_{i+1j+1}, P_{ij}, P_{i+1j}) \\ f_{ij} & H_0(\phi_{ij}, \phi_{i+1j}, \phi_{i+1j+1}, P_{ij}, P_{i+1j}, P_{i+1j+1}) \\ +f_{ij+1} & H_0(\phi_{ij+1}, \phi_{ij}, \phi_{i+1j+1}, P_{ij+1}, P_{ij}, P_{i+1j+1}) \\ +f_{i+1j+1} & H_0(\phi_{i+1j+1}, \phi_{ij}, \phi_{i+1j}, P_{i+1j+1}, P_{ij}, P_{i+1j}) \end{pmatrix}$$

Since in virtue of Eq. (1), the approximation of  $\int_{\Omega} f \, d\Omega$  is to be  $\sum_{ij} f_{ij} H_{ij} \Delta x \Delta y$ , we obtain the following second-order accurate approximation of the multi-dimensional Heaviside function by collecting all the coefficients in front of  $f_{ij}$ :

$$H_{ij} = \frac{1}{\Delta x \Delta y} \begin{pmatrix} H_0(P_{ij}, P_{i+1j}, P_{i+1j+1}, \phi_{ij}, \phi_{i+1j}, \phi_{i+1j+1}) \\ + H_0(P_{ij}, P_{ij+1}, P_{i+1j+1}, \phi_{ij}, \phi_{ij+1}, \phi_{i+1j+1}) \\ + H_0(P_{ij}, P_{i-1j}, P_{i-1j-1}, \phi_{ij}, \phi_{i-1j}, \phi_{i-1j-1}) \\ + H_0(P_{ij}, P_{ij-1}, P_{i-1j-1}, \phi_{ij}, \phi_{ij-1}, \phi_{i-1j-1}) \\ + H_0(P_{ij}, P_{i+1j}, P_{ij-1}, \phi_{ij}, \phi_{i+1j}, \phi_{ij-1}) \\ + H_0(P_{ij}, P_{i-1j}, P_{ij+1}, \phi_{ij}, \phi_{i-1j}, \phi_{ij+1}) \end{pmatrix}.$$

Similarly, using Eq. (2), we obtain the following second-order accurate discretization of the delta function:

$$\delta_{ij} = \frac{1}{\Delta x \Delta y} \begin{pmatrix} \delta_0(P_{ij}, P_{i+1j}, P_{i+1j+1}, \phi_{ij}, \phi_{i+1j}, \phi_{i+1j+1}) \\ + \delta_0(P_{ij}, P_{ij+1}, P_{i+1j+1}, \phi_{ij}, \phi_{ij+1}, \phi_{i+1j+1}) \\ + \delta_0(P_{ij}, P_{i-1j}, P_{i-1j-1}, \phi_{ij}, \phi_{i-1j}, \phi_{i-1j-1}) \\ + \delta_0(P_{ij}, P_{ij-1}, P_{i-1j-1}, \phi_{ij}, \phi_{ij-1}, \phi_{i-1j-1}) \\ + \delta_0(P_{ij}, P_{i+1j}, P_{ij-1}, \phi_{ij}, \phi_{i+1j}, \phi_{ij-1}) \\ + \delta_0(P_{ij}, P_{i-1j}, P_{ij+1}, \phi_{ij}, \phi_{i-1j}, \phi_{ij+1}) \end{pmatrix}.$$

### 3.2. Three spatial dimensions

The previous discretizations can be extended to three spatial discretization in a straightforward manner: first, we evaluate the integrals  $\int_{\Omega} f \, d\Omega$  and  $\int_{\Gamma} f \, d\Gamma$  using the integration method described in Section 3. These formulas involve the contribution of the 20 tetrahedra neighboring each grid node  $(i, j, k)$  (see Table 3). Then using formulas (1) and (2), one can define the approximation of the multi-dimensional Heaviside and delta functions in three spatial dimensions as

$$H_{i,j,k} = \frac{1}{\Delta x \Delta y \Delta z} \sum_{\Delta P_a P_b P_c P_d \text{ neighboring tetrahedron of } (i,j,k)} H_0(P_a, P_b, P_c, P_d, \phi_a, \phi_b, \phi_c, \phi_d)$$

and

$$\delta_{i,j,k} = \frac{1}{\Delta x \Delta y \Delta z} \sum_{\Delta P_a P_b P_c P_d \text{ neighboring tetrahedron of } (i,j,k)} \delta_0(P_a, P_b, P_c, P_d, \phi_a, \phi_b, \phi_c, \phi_d),$$

where the  $\Delta P_a P_b P_c P_d$ 's are defined in Table 3.

## 4. Numerical examples

In this section, we provide numerical evidence that our method is second-order accurate in the  $L^\infty$ -norm in two and three spatial dimensions. Since the discretizations we propose in this paper are heavily based on the geometric integration of [12],

**Table 3**  
List of the 20 tetrahedra  $\Delta P_a P_b P_c P_d$  neighboring each vertex  $(i, j, k)$

$P_a$	$P_b$	$P_c$	$P_d$
$(i, j, k)$	$(i + 1, j, k)$	$(i, j + 1, k)$	$(i, j, k + 1)$
$(i, j, k)$	$(i + 1, j, k)$	$(i, j, k - 1)$	$(i, j - 1, k)$
$(i, j, k)$	$(i, j, k - 1)$	$(i, j + 1, k)$	$(i - 1, j, k)$
$(i, j, k)$	$(i, j - 1, k)$	$(i - 1, j, k)$	$(i, j, k + 1)$
$(i, j, k)$	$(i, j - 1, k - 1)$	$(i - 1, j, k - 1)$	$(i - 1, j - 1, k)$
$(i, j, k)$	$(i, j - 1, k - 1)$	$(i - 1, j, k - 1)$	$(i, j, k - 1)$
$(i, j, k)$	$(i, j - 1, k - 1)$	$(i, j - 1, k)$	$(i - 1, j - 1, k)$
$(i, j, k)$	$(i - 1, j, k)$	$(i - 1, j, k - 1)$	$(i - 1, j - 1, k)$
$(i, j, k)$	$(i - 1, j, k)$	$(i - 1, j + 1, k)$	$(i - 1, j, k + 1)$
$(i, j, k)$	$(i, j + 1, k + 1)$	$(i - 1, j + 1, k)$	$(i - 1, j, k + 1)$
$(i, j, k)$	$(i, j + 1, k + 1)$	$(i - 1, j + 1, k)$	$(i, j + 1, k)$
$(i, j, k)$	$(i, j + 1, k + 1)$	$(i, j, k + 1)$	$(i - 1, j, k + 1)$
$(i, j, k)$	$(i + 1, j - 1, k)$	$(i, j - 1, k)$	$(i, j - 1, k + 1)$
$(i, j, k)$	$(i + 1, j - 1, k)$	$(i + 1, j, k + 1)$	$(i, j - 1, k + 1)$
$(i, j, k)$	$(i + 1, j - 1, k)$	$(i + 1, j, k + 1)$	$(i + 1, j, k)$
$(i, j, k)$	$(i, j, k + 1)$	$(i + 1, j, k + 1)$	$(i, j - 1, k + 1)$
$(i, j, k)$	$(i + 1, j, k - 1)$	$(i, j + 1, k - 1)$	$(i, j, k - 1)$
$(i, j, k)$	$(i + 1, j, k - 1)$	$(i, j + 1, k - 1)$	$(i + 1, j + 1, k)$
$(i, j, k)$	$(i + 1, j, k - 1)$	$(i + 1, j, k)$	$(i + 1, j + 1, k)$
$(i, j, k)$	$(i, j + 1, k)$	$(i, j + 1, k - 1)$	$(i + 1, j + 1, k)$

we do not provide examples demonstrating the robustness of the method but we stress that this method inherits from this property, as demonstrated in [12]. In these examples  $h$  is the spacing between grid nodes.

4.1. Computing lengths and areas in two spatial dimensions

Consider an irregular domain  $\Omega$  represented in the polar coordinates as  $r \leq 1 + \frac{1}{2} \cos(5\theta)$  with a corresponding level set function  $\phi(x, y) = 2(x^2 + y^2)^3 - 2(x^2 + y^2)^2 \sqrt{x^2 + y^2} - (x^5 + 5xy^4 - 10x^3y^2)$ . We measure its area and arc length using the discretizations of Heaviside and delta function, respectively. The exact area is  $\frac{9}{8}\pi$ , and the arc length is approximately 12.329044714372... Table 4 demonstrates the second-order accuracy of our approach as we refine the grid.

4.2. Computing surfaces and volumes in three spatial dimensions

Consider an ellipsoid defined by  $\frac{x^2}{1.5^2} + \frac{y^2}{.75^2} + \frac{z^2}{.5^2} = 1$  on a computational domain  $[-1.6, 1.6] \times [-.8, .8] \times [-.6, .6]$ . Its surface area is approximately 9.901821... and its volume is  $\frac{3}{4}\pi$ , as detailed in [20]. Table 5 demonstrates second-order accuracy of our method when computing its surface area and volume using our discretizations of the Heaviside and the delta functions.

4.3. Evaluation of source terms on irregular domain

In the case of the computation of lengths, areas and volumes, the integrand is identically equal to one, so the domain of definition of the integrand is irrelevant. In the case of evaluating singular source terms, the integrand may not be constant and may be defined only in the interior of the irregular domain. In this example, we show that a simple extrapolation of the integrand allow to define it at all grid points near the interface; and subsequent use of our approximation of the delta Dirac function produces second-order accuracy in the  $L^\infty$ -norm: consider a domain  $\Omega$  to be the unit circle with center (0,0) and a quantity  $f(x, y) = e^{-x^2 - y^2}$  defined only inside this irregular domain. Outside the domain, we take  $f(x, y) = 0$ . The integral value  $\int_\Omega f = \pi(1 - 1/e)$  is approximated by our discretization of the multi-dimensional Heaviside function after extrapolating quadratically  $f$  using method described in [1,13]. Fig. 5 depicts the contours of  $f(x, y)$  before and after the extrapolation. Table 6 demonstrates second-order accuracy in the  $L^\infty$ -norm (see Fig. 6).

**Table 4**  
Convergence analysis in computing the area and arc length of the irregular domain defined by  $r \leq 1 + \frac{1}{2} \cos(5\theta)$  using the proposed Heaviside and delta functions

$\Delta x = \Delta y$	$\ A - A_h\ _\infty$	Rate	$\ L - L_h\ _\infty$	Rate
0.15	$9.02 \times 10^{-2}$		$4.29 \times 10^{-1}$	
0.075	$2.31 \times 10^{-2}$	1.97	$1.35 \times 10^{-1}$	1.67
0.0375	$5.35 \times 10^{-3}$	2.11	$3.32 \times 10^{-2}$	2.02
0.01875	$1.35 \times 10^{-3}$	1.99	$6.71 \times 10^{-3}$	2.31
0.009375	$3.31 \times 10^{-4}$	2.03	$1.48 \times 10^{-3}$	2.19

**Table 5**

Convergence analysis in computing the volume and the surface area of an ellipsoid using the proposed Heaviside and delta functions

$\Delta x = \Delta y = \Delta z$	$\ V - V_h\ _\infty$	Rate	$\ S - S_h\ _\infty$	Rate
0.2	$1.44 \times 10^{-1}$		$3.14 \times 10^{-1}$	
0.1	$3.66 \times 10^{-2}$	1.98	$7.85 \times 10^{-2}$	2.00
0.05	$9.16 \times 10^{-3}$	1.99	$1.95 \times 10^{-2}$	2.00
0.025	$2.29 \times 10^{-3}$	2.00	$4.89 \times 10^{-3}$	2.00
0.0125	$5.72 \times 10^{-4}$	2.00	$1.22 \times 10^{-3}$	2.00

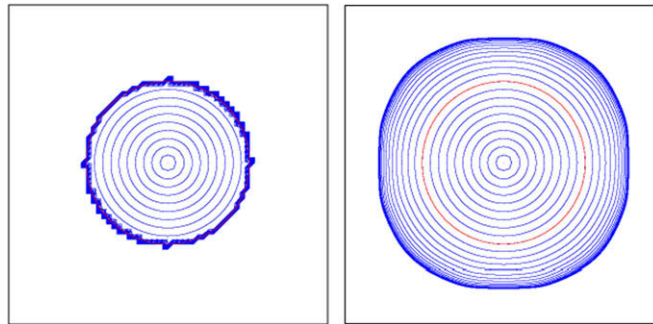


**Fig. 5.** Contours of  $f(x, y)$  before (left) and after (right) the quadratic extrapolation of example 4.3. The red contour represents the domain's boundary  $\partial\Omega$ .

**Table 6**

Convergence analysis in computing the integral of Example 4.3

$\Delta x = \Delta y$	$\ I - I_h\ _\infty$	Rate
0.125	$8.69 \times 10^{-2}$	
0.0625	$1.28 \times 10^{-2}$	2.76
0.03125	$2.59 \times 10^{-3}$	2.30
0.015625	$6.35 \times 10^{-4}$	2.02
0.0078125	$1.56 \times 10^{-4}$	2.02

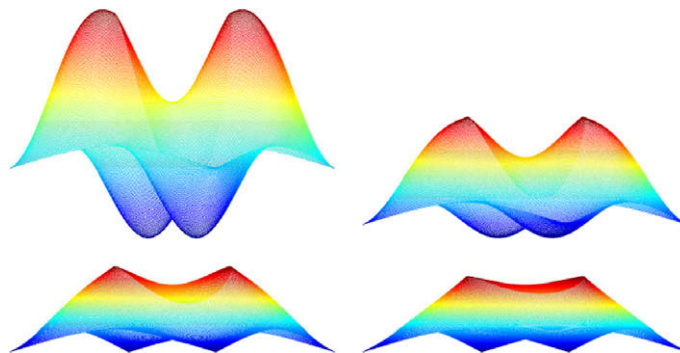


**Fig. 6.** Evolution of the solution to the heat equation with singular source term of Section 4.5. From left to right and top to bottom,  $t = 0$ ,  $t = .039$ ,  $t = .078$  and  $t = .125$  demonstrating a kink in the solution on  $\Gamma$ .

4.4. Poisson equation with a singular source term

Consider the Poisson equation studied in [4].

$$-\Delta u(x) = \delta_\Gamma(x) \quad \text{in } \Omega,$$

$$u(x) = 1 - \frac{\ln(2|x|)}{2} \quad \text{on } \partial\Omega,$$

where  $\Omega = [-1, 1] \times [-1, 1]$  and  $\Gamma = \{x \in \mathbb{R}^2 \mid |x| = \frac{1}{2}\}$ . The equation has the following solution:



**Table 7**  
Accuracy of the Poisson problem 4.4. The exact solution has a kink at the interface  $\Gamma$

Grid	$\ u - u_h\ _\infty$	Rate	$\ u - u_h\ _\infty$ in $\tilde{\Omega}_{2\Delta x}$	Rate	$\ u - u_h\ _\infty$ in $\tilde{\Omega}_2$	Rate	$\ u - u_h\ _1$	Rate
$32^2$	$7.35 \times 10^{-3}$		$8.18 \times 10^{-4}$		$4.14 \times 10^{-4}$		$3.09 \times 10^{-4}$	
$64^2$	$3.02 \times 10^{-3}$	1.27	$4.43 \times 10^{-4}$	0.88	$9.93 \times 10^{-5}$	2.06	$8.07 \times 10^{-5}$	1.93
$128^2$	$2.53 \times 10^{-3}$	0.26	$1.91 \times 10^{-4}$	1.21	$2.46 \times 10^{-5}$	2.00	$2.25 \times 10^{-5}$	1.84
$256^2$	$1.22 \times 10^{-3}$	1.05	$7.98 \times 10^{-5}$	1.25	$6.39 \times 10^{-6}$	1.94	$5.83 \times 10^{-6}$	1.94
$512^2$	$6.78 \times 10^{-4}$	0.84	$3.17 \times 10^{-5}$	1.32	$1.59 \times 10^{-6}$	2.00	$1.51 \times 10^{-6}$	1.94
$1024^2$	$3.36 \times 10^{-4}$	1.01	$1.31 \times 10^{-5}$	1.27	$4.03 \times 10^{-7}$	1.98	$3.78 \times 10^{-7}$	1.99

**Table 8**  
Accuracy of the heat equation problem 4.5 at  $t = 0.125$

Grid	$\ u - u_h\ _\infty$	Rate	$\ u - u_h\ _\infty$ in $\tilde{\Omega}_{2\Delta x}$	Rate	$\ u - u_h\ _\infty$ in $\tilde{\Omega}_2$	Rate	$\ u - u_h\ _1$	Rate
$32^2$	$2.76 \times 10^{-2}$		$2.76 \times 10^{-2}$		$2.76 \times 10^{-2}$		$1.05 \times 10^{-2}$	
$64^2$	$6.52 \times 10^{-3}$	2.08	$6.52 \times 10^{-3}$	2.08	$6.52 \times 10^{-3}$	2.08	$2.57 \times 10^{-3}$	2.03
$128^2$	$1.83 \times 10^{-3}$	1.82	$1.60 \times 10^{-3}$	2.02	$1.60 \times 10^{-3}$	2.02	$6.46 \times 10^{-3}$	1.99
$256^2$	$6.03 \times 10^{-4}$	1.60	$4.00 \times 10^{-4}$	2.00	$4.00 \times 10^{-4}$	2.00	$1.62 \times 10^{-4}$	1.99
$512^2$	$2.62 \times 10^{-4}$	1.20	$1.19 \times 10^{-5}$	1.74	$9.97 \times 10^{-5}$	2.00	$4.07 \times 10^{-4}$	1.99
$1024^2$	$1.10 \times 10^{-4}$	1.24	$3.96 \times 10^{-5}$	1.58	$2.49 \times 10^{-5}$	2.00	$1.02 \times 10^{-5}$	1.99

The exact solution has a kink at the interface  $\Gamma$ .

$$u(\mathbf{x}) = \begin{cases} 1 & \text{if } |\mathbf{x}| \leq \frac{1}{2} \\ 1 - \frac{\ln(2|\mathbf{x}|)}{2} & \text{if } |\mathbf{x}| \geq \frac{1}{2} \end{cases}$$

On a uniform grid, we discretize the Laplace operator with standard central finite differences and the multi-dimensional delta function  $\delta_r$  with the method presented above. We follow the notation of [23] and define  $\tilde{\Omega}_\beta = \{\mathbf{x} : \mathbf{x} \in \Omega, |d(\Gamma, \mathbf{x})| > \beta\}$ . Table 7 shows that our discretization produces results that are second-order accurate in the  $L^1$  norm and first-order accurate in the  $L^\infty$  norm with the expected drop in accuracy near the interface since the solution presents a kink. Table 7 also demonstrates second-order accuracy in the  $L^\infty$  norm when the accuracy is computed away from the interface, i.e. we take  $\beta > 0.2$  as in [4].

We note that a finite volume approach for discretizing the PDE would be more consistent with our derivation of the delta and Heaviside functions, but we seek to demonstrate that our discretizations can easily be applied in a finite difference setting.

#### 4.5. Heat equation with a singular source term

Consider the following PDE:

$$\begin{aligned} u_t &= \Delta u + \delta_\Gamma \quad \text{in } \Omega, \\ u(\mathbf{x}, t) &= 1 - \frac{\ln(2|\mathbf{x}|)}{2} \quad \text{on } \partial\Omega, \\ u(\mathbf{x}, 0) &= 1 - \frac{\ln(2|\mathbf{x}|)}{2} \quad \text{in } \Omega, \end{aligned}$$

where  $\Omega = [-1, 1] \times [-1, 1]$  and  $\Gamma = \{\mathbf{x} \in \mathbb{R}^2 \mid |\mathbf{x}| = \frac{1}{2}\}$ . The equation has the following solution:

$$u(\mathbf{x}, t) = \begin{cases} e^{-2\pi^2 t} \sin(\pi x) \sin(\pi y) + 1 & \text{if } |\mathbf{x}| \leq \frac{1}{2} \\ e^{-2\pi^2 t} \sin(\pi x) \sin(\pi y) + 1 - \frac{\ln(2|\mathbf{x}|)}{2} & \text{if } |\mathbf{x}| \geq \frac{1}{2} \end{cases}$$

On a uniform grid, we discretize the time derivative with the Crank–Nicolson method, the Laplace operator with standard central finite differences, and the multi-dimensional delta function  $\delta_r$  with our method.

Table 8 shows that our discretization produces second-order accurate results in the  $L^1$  norm first-order accurate solution in the  $L^\infty$  norm. Table 8 also demonstrates that the solution is second-order accurate in the  $L^\infty$  norm if one excludes the nodes near the singularity.

### 5. Conclusion

We have introduced a second-order accurate method for the discretization of the multi-dimensional Heaviside and delta functions on irregular domains in two and three spatial dimensions and have provided numerical examples to illustrate the accuracy. This method leverages on geometric integrations that are robust to the perturbation of the interface's location on

the grid and therefore naturally inherits this property. We use a level set function for the description of the irregular domain's boundary but this approach is not limited to level set simulations since distance functions can be readily constructed from any representation of irregular domains. The discretizations only depend on the level function and not on its derivatives, and are therefore robust to numerical noise. In addition, since our discretizations are cell-based, they can be trivially extended to unstructured grids as in [10–12]. We have also presented examples of partial differential equations with singular source terms and showed that the direct discretization of the singular source term together with standard finite differences lead second-order accuracy in the  $L^1$  norm, first-order accuracy in  $L^\infty$  in the whole domain, and second-order accuracy in  $L^\infty$  away from the support of the singular source.

## Acknowledgments

The research of C. Min was supported in part by the Kyung Hee University Research Fund (KHU-20070608) in 2007. The research of F. Gibou was supported in part by a Sloan Research Fellowship in Mathematics, by NSF under Grant agreement DMS 0713858 and by the DOE Office of Science under Grant No. DE-FG02-08ER15991.

## References

- [1] T. Aslam, A partial differential equation approach to multidimensional extrapolation, *J. Comput. Phys.* 193 (2004) 349–355.
- [2] J.U. Brackbill, D.B. Kothe, C. Zemach, A continuum method for modelling surface tension, *J. Comput. Phys.* 100 (1992) 335–353.
- [3] D. Calhoun, P. Smereka. The numerical approximation of a delta function. Preprint <<http://www.math.lsa.umich.edu/~psmerek/notes.html>>, 2004.
- [4] B. Engquist, A.K. Tornberg, R. Tsai, Discretization of Dirac delta functions in level set methods, *J. Comput. Phys.* 207 (2005) 28–51.
- [5] D. Enright, R. Fedkiw, J. Ferziger, I. Mitchell, A hybrid particle level set method for improved interface capturing, *J. Comput. Phys.* 183 (2002) 83–116.
- [6] J.E. Goodman, J. O'Rourke, *The handbook of discrete and computational geometry*, CRC Press LL, 1997.
- [7] A. Karma, W.-J. Rappel, Quantitative phase-field modeling of dendritic growth in two and three dimensions, *Phys. Rev. E* 57 (1997) 4323–4349.
- [8] H.W. Kuhn, Some combinational lemmas in topology, *IBM J. Res. Develop.* 4 (1960) 508–524.
- [9] A. Mayo, The fast solution of Poisson's and the biharmonic equations on irregular regions, *SIAM J. Numer. Anal.* 21 (1984) 285–299.
- [10] C. Min, Simplicial isosurfacing in arbitrary dimension and codimension, *J. Comput. Phys.* 190 (2003) 295–310.
- [11] C. Min, Local level set method in high dimension and codimension, *J. Comput. Phys.* 200 (2004) 368–382.
- [12] C. Min, F. Gibou, Geometric integration over irregular domains with application to level set methods, *J. Comput. Phys.* 226 (2007) 1432–1443.
- [13] C. Min, F. Gibou, A second order accurate level set method on non-graded adaptive Cartesian grids, *J. Comput. Phys.* 225 (2007) 300–321.
- [14] S. Osher, R. Fedkiw, *Level Set Methods and Dynamic Implicit Surfaces*, Springer-Verlag, New York, NY, 2002.
- [15] C. Peskin, The immersed boundary method, *Acta Numer.* 11 (2002) 479–517.
- [16] J.F. Sallee, The middle-cut triangulations of the n-cube, *SIAM J. Alg. Disc. Methods* 5 (1984) 407–419.
- [17] J. Sethian, Fast marching methods, *SIAM Rev.* 41 (1999) 199–235.
- [18] J.A. Sethian, *Level Set Methods and Fast Marching Methods*, Cambridge University Press, Cambridge, 1999.
- [19] P. Smereka, Semi-implicit level set methods for curvature and surface diffusion motion, *J. Sci. Comput.* 19 (2003) 439–456.
- [20] P. Smereka, The numerical approximation of a delta function with application to level set methods, *J. Comput. Phys.* 211 (2006) 77–90.
- [21] M. Sussman, E.G. Puckett, A coupled level set and volume-of-fluid method for computing 3d and axisymmetric incompressible two-phase flows, *J. Comput. Phys.* 162 (2000) 301–337.
- [22] M. Sussman, P. Smereka, S. Osher, A level set approach for computing solutions to incompressible two-phase flow, *J. Comput. Phys.* 114 (1994) 146–159.
- [23] A.-K. Tornberg, B. Engquist, Numerical approximations of singular source terms in differential equations, *J. Comput. Phys.* 200 (2004) 462–488.
- [24] J. Towers, Two methods for discretizing a delta function supported on a level set, *J. Comput. Phys.* 220 (2007) 915–931.
- [25] J. Towers, A convergence rate theorem for finite difference approximations to delta functions, *J. Comput. Phys.* 227 (2008) 6591–6597.
- [26] G. Tryggvason, B. Bunner, A. Esmaeeli, D. Juric, N. Al-Rawahi, W. Tauber, J. Han, S. Nas, Y.-J. Jan, A front-tracking method for the computations of multiphase flow, *J. Comput. Phys.* 169 (2001) 708–759.
- [27] J. Walén, On the approximation of singular source terms in differential equations, *Numer. Methods Partial Differ. Equat.* 15 (1999) 503–520.